

Coronal Response of Bi-directional Jets

J.G. Doyle

Armagh Observatory, College Hill, Armagh BT61 9DG, N. Ireland

M.S. Madjarska

Armagh Observatory, College Hill, Armagh BT61 9DG, N. Ireland

now at: Mullard Space Science Laboratory, UCL, Holmbury St. Mary, Dorking, Surrey, RH5 6NT, UK

E. Dzifčáková

Astronomical Institute, Faculty of Mathematics, Physics and Informatics, Comenius University, Mlynská dolina, 842 48 Bratislava 4, Slovakia

I.E. Dammasch

Mullard Space Science Laboratory, UCL, Holmbury St. Mary, Dorking, Surrey, RH5 6NT, UK

Abstract. EUV bi-directional jets are a prominent class of phenomena characterizing the solar transition region. Using simultaneously obtained SUMER observations in the chromospheric Si II 1251.16 Å and C I 1251.17 Å, transition region N V 1238.8 Å and coronal Mg X 625 Å lines we show an example of a bi-directional jet registered in the chromospheric and the transition region lines but not showing any detectable signature in the coronal line. The phenomenon, however, was also clearly detected by the TRACE imager with the 171 Å filter. This discrepancy is explained here with a non-Maxwellian electron distribution which makes a significant fraction of the plasma in the TRACE 171 Å pass-band to be derived from temperatures around $\approx 300,000\text{K}$, as opposed to $\approx 800,000\text{K}$. This could have implications for other phenomena observed in the TRACE pass-bands, including the transition region ‘moss’ and the 3 and 5 mins oscillations.

Keywords: Sun: Transition region–Ultraviolet: SoHO–Sun: bi-directional jets: coronal signature: Non-Maxwellian: Kappa distribution.

1. Introduction

The location and importance of ultraviolet bi-directional jets, often called ‘explosive events’, within the wider frame-work of the upper solar atmosphere is still uncertain. These dynamic events were first detected to occur in the transition region with a birthrate over the whole Sun of between 600 s^{-1} (Dere, Bartoe & Brueckner 1989) and 3300 s^{-1} (Rytova & Tarbell 2000). They are characterized by spatial scales of $\approx 2000\text{ km}$, average lifetime of about 200 s and have highly non-Gaussian line profiles with Doppler shifts up to 250 km s^{-1} (Dere, Bartoe & Brueckner 1989) and often appear in bursts lasting several minutes (Innes *et al.* 1997; Chae *et al.* 1998; Pérez *et al.* 1999).



© 2004 Kluwer Academic Publishers. Printed in the Netherlands.

Madjarska & Doyle (2002) provided evidence that bi-directional jets also appear in chromospheric lines such as O I and the optically thick H I Ly 6, 7, 8, 9 and 10 lines. The results of an attempt to observe the coronal counterparts to bi-directional jets were presented by Dere (1994), Moses & Cook (1994) and Teriaca, Madjarska & Doyle (2002). The latter authors obtained high spectral resolution data for a large event in the transition region line N v 1238 Å and the coronal line Mg x 625 Å. These authors concluded that the event observed in N v showed a small enhancement in Mg x which is however caused by the presence of a close-by blend from a Si II line (see Teriaca, Madjarska & Doyle 2002 for further details on this blend).

The above spectroscopic based studies are however at odds with TRACE studies. The TRACE mission was designed to obtain high quality images of the solar transition region and corona in order to explore the connection between the photospheric magnetic field and the associated hot structures in the upper atmosphere. The TRACE images have a resolution of one arcsecond. Its passbands are set to cover Fe IX, X, XII and XV lines in the EUV, while additional filters allow observations over a broad spectral region centered at C IV 1550 Å, H I Ly α , and the UV continuum (see Handy *et al.* 1999; Schrijver *et al.* 1999).

In a joint SUMER/TRACE study by Winebarger, Updike & Reeves (2002), significant fluctuations were found in the TRACE 171 Å passband in 35% of the pixels which show enhanced wings in the transition region line C IV 1548 Å (observed with SUMER) over an area within an active region. Also, Erdélyi, De Pontieu & Sarro (1999) reported a bi-directional jet observed with SUMER in the N v 1238 Å transition region line, plus simultaneous detection in the TRACE 171 Å image.

Here, we offer an explanation for this apparent discrepancy in terms of a non-Maxwellian electron distribution. In Sect. 2 & 3 we describe the SUMER and TRACE observations plus the data analysis and results. In Sect. 4 we show the effect of a non-Maxwellian electron distribution on the ionization balance of Fe IX and X. In Sect. 5, we generate synthetic spectra in the 165 to 215 Å region by folding in the differential emission measure curve in order to find the relative line contributions to narrow-band filters, such as TRACE 171 Å. Some brief remarks and suggestions for possible implications and future work are given in Sect. 6.

2. Observations

The SUMER (for details see Wilhelm *et al.* 1995; 1997; Lemaire *et al.* 1997) data were obtained on 1999 June 1 pointing the instrument at

active region AR 8552. The observations were obtained at coordinates Solar_X = 409'' and Solar_Y = 400'' compensating for the solar rotation with a step size of 0.75'' after each 13 spectra. The 1'' \times 120'' slit was used on detector B. The observations started at 09:13 UT and ended at 11:02 UT, consisting of a temporal sequence of five spectral windows (120 spatial \times 50 spectral pixels) centered on N v 1238.82 Å, N v 1242.82 Å, Si II 1251.16 Å, O v 629.73 Å and Mg x 624.94 Å (the last two lines observed in second order) using an exposure time of 25 s. Based on the ionization balance calculations of Mazzotta *et al.* (1998), Si II, N v, O v and Mg x have peak formation temperatures around 12,500 K, 200,000 K, 250,000 K and 1,250,000 K respectively.

TRACE 171 Å images discussed here were obtained starting at 09:02 UT and finishing at 12:00 UT. The integration time of each image was 5.8 s from 09:02 UT until 09:41 UT and 4.1 s after that time. Each image is divided by the exposure time. The images were taken every 12 s. We discuss here only the data which were obtained simultaneously with the SUMER spectrometer. In addition, white-light images were obtained every 12 min starting at 09:22 UT. The instrument was pointed at coordinates Solar_X = 422'' and Solar_Y = 401''. TRACE images have a pixel size of 0''.5 which gives a spatial resolution of 1''. A preliminary discussion of this data was given by Erdélyi, De Pontieu & Sarro (1999).

3. Data analysis and results

3.1. SUMER & TRACE DATA

A transient phenomenon was recorded simultaneously by the SUMER spectrometer on-board SoHO and the TRACE imager on 1999 June 1. It consisted of numerous bi-directional jets as seen by the SUMER spectrometer. The strongest event, which is the subject of the present study, shows Doppler shifts up to 200 km s⁻¹. The event is seen in two SUMER spectra and two TRACE images.

The data analysis started with a de-rotation of the TRACE images (rotational compensation was applied to the SUMER observations) and an alignment of the two instruments. Both instruments have a pointing offset which was first evaluated using the known offset for the particular wavelength range. Simultaneously obtained data with the Coronal Diagnostic Spectrograph (CDS) (Harrison *et al.* 1995) in the Mg IX 368 Å line with the same pointing as SUMER was used to make a more precise alignment. The intensity images in the coronal CDS Mg IX 368 Å, SUMER Mg x 625 Å and TRACE 171 Å were visually aligned using

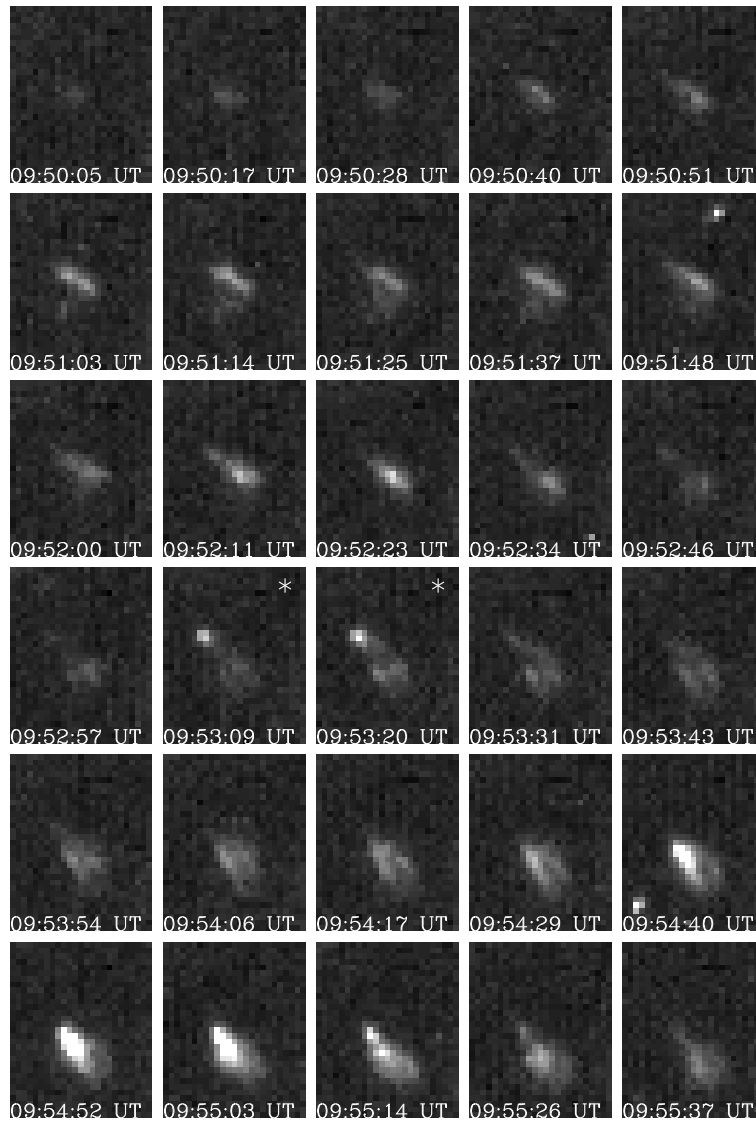


Figure 1. TRACE 171 Å images showing a transient event. The strong bi-directional jet is registered in the co-spatial and co-temporal SUMER spectra that are associated with the two TRACE images shown with an asterisk in the upper right corner.

a long-lived bright coronal structure as reference. Finally the temporal evolution of the event was visually analysed in the SUMER and TRACE data (Fig. 1). It revealed that the event as seen in the TRACE data

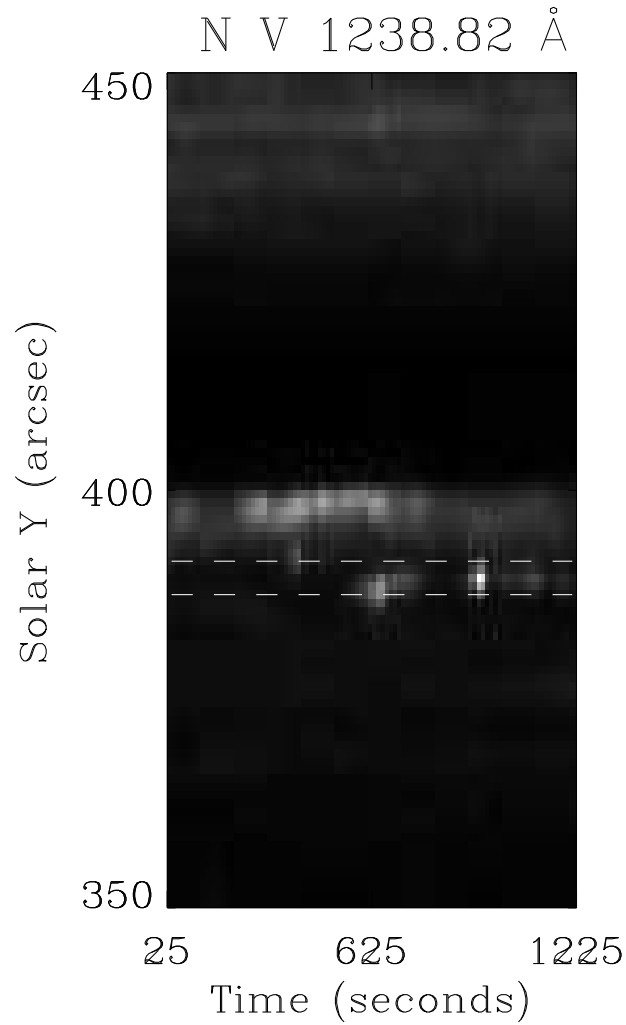


Figure 2. N V intensity map. The horizontal dashed lines define the portion of the slit along which the bi-directional jet was seen.

appears along the SUMER slit at the position shown with dashed lines in Fig. 2. That helped us to align the two datasets with a precision of $1''$. The bi-directional jet spectral line profile is shown in Fig. 3.

3.2. LINE BLENDS

The Mg x 625 Å line was observed by the SUMER spectrometer as a second order line at 1249.90 Å (Curdt *et al.* 2001). Therefore, it over-

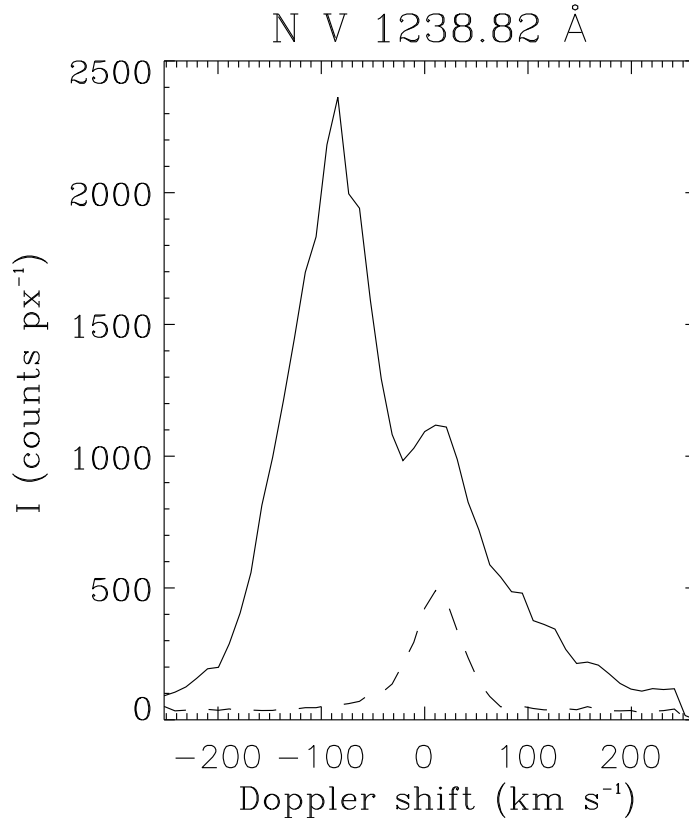


Figure 3. The N v 1238 Å line profile before (dashed line) and during the event (solid line).

laps with several first order chromospheric lines such as P II 1249.82, Mg II 1249.93 and Si II 1250.09. In the present observations the Mg x line was recorded on the KBr part of detector B. The SUMER detectors A and B have photo-cathode areas with different response where the central part has a coating of potassium bromide (KBr) while the other parts use a (bare) micro-channel plate. Second order lines are less sensitive to the KBr coating and hence the effects of first order line blends will increase significantly when recorded on KBr. A detailed discussion on these blends is given by Teriaca, Madjarska & Doyle (2002). In their paper, a Si II contribution of 1-2% in the quiet Sun and $\approx 5\%$ during their observed bi-directional jet was determined for a spectrum recorded on the bare part of the detector. They also made a suggestion on the total contribution of all blending lines when recorded

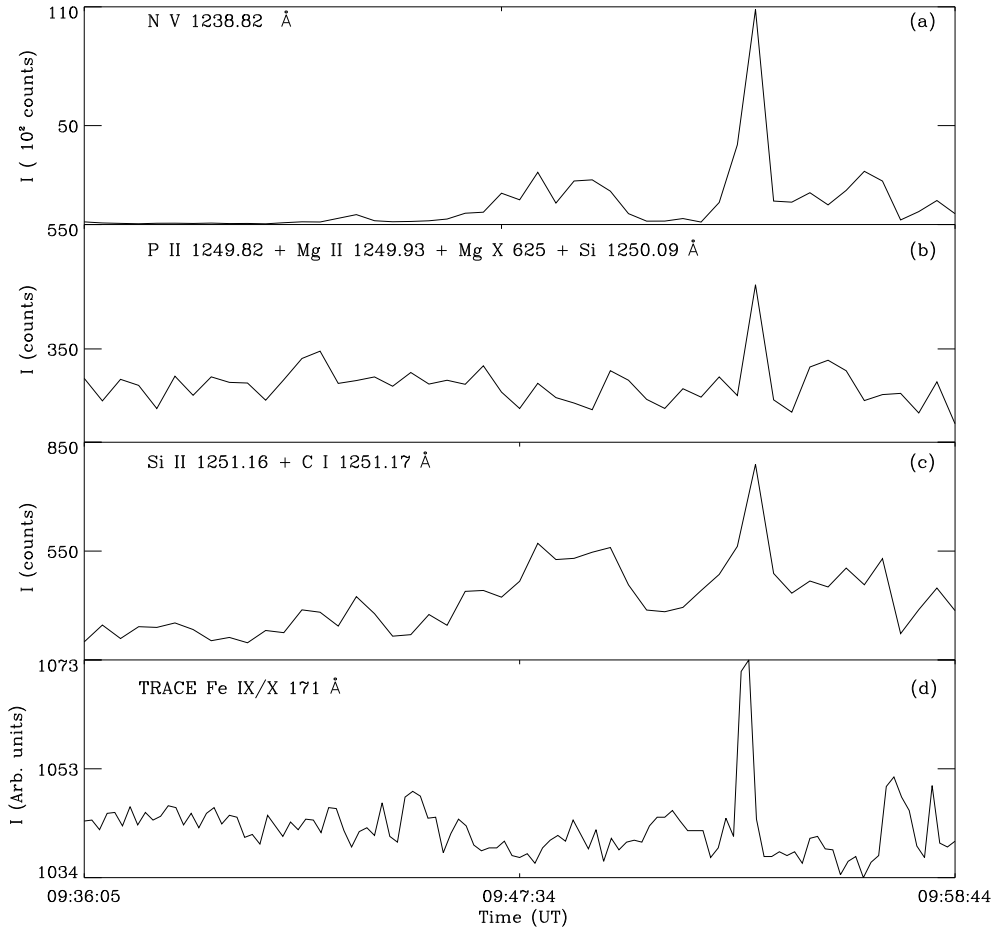


Figure 4. From top to bottom: (a) The temporal behaviour of the integrated radiance in the blue wing of N v 1238 Å; (b) the total intensity in the feature at 1249.90 Å comprising of Mg x 625 Å(2), Si II 1250.09 Å, P II 1249.82 Å and Mg II 1240.93 Å, (c) Si II 1251.16 + C I 1251.17 Å and (d) TRACE Fe IX/x 171 Å window.

on the KBr part of the detector which should be 10 - 15% in quiet Sun observations.

We performed a detailed spectroscopic analysis in order to estimate the contribution of the spectral lines blending the Mg x line when recorded on the KBr part of detector B. A Gauss fit was applied to all registered spectral lines for each spectrum obtained at the same

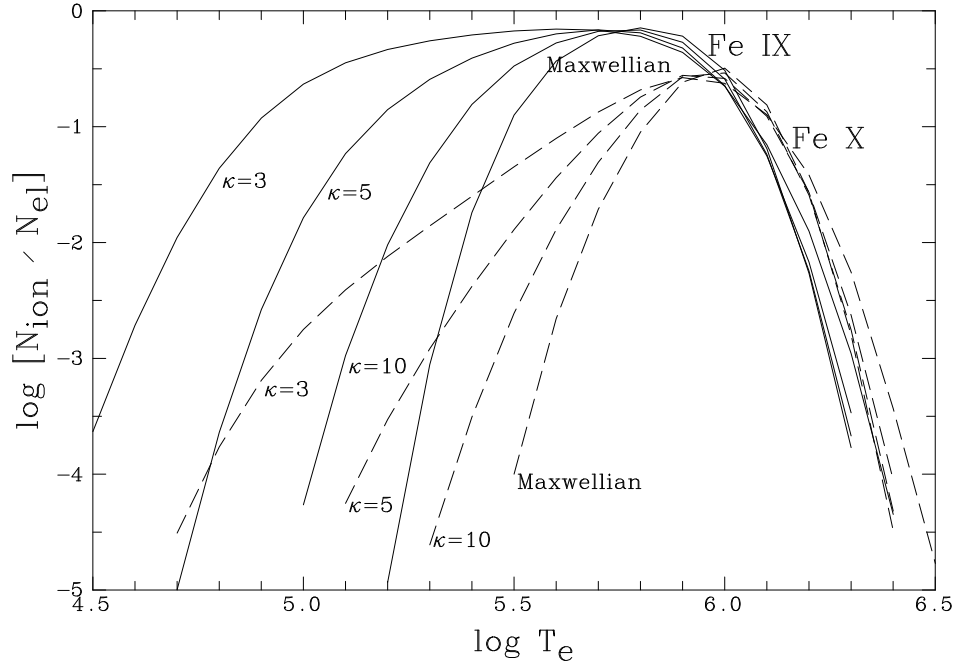


Figure 5. Ionization fractions for Fe IX and Fe X assuming a Maxwellian electron distribution plus a Kappa distribution for $\kappa = 3, 5$ & 10 .

position along the slit where the event took place. In some cases a constrained profile (a fixed line width and/or line position) had to be applied. The average contribution for the Si II 1250.09 Å line was found to be between 35 and 40 %. Another few percent can come from the Mg II and the P II lines leading to a total first-order contribution of $\approx 40\%$.

3.3. RESULTS

In Fig. 4(a) we show the radiance temporal variations obtained by integrating over 8 spectral pixels (0.3 Å) in the blue wing of N V and 5 spatial pixels along the SUMER slit as indicated by the dashed lines in Fig. 2. The event has a very strong blue wing as seen in Fig. 3 and the strongest intensity and velocity increase are concentrated in a single spatial pixel (1'') (Fig. 2). Fig. 4(b) represents the radiance in the feature at 1249.90 Å which includes the 2nd order Mg X 625 Å line plus lines contribution from Si II 1250.09 Å, Mg II 1249.93 Å and P II 1240.82 Å. Fig. 4(c) shows the integrated radiance in Si II 1251.16 blended with C I 1251.17 (Curdt *et al.* 2001). The continuum background is removed in all radiance plots.

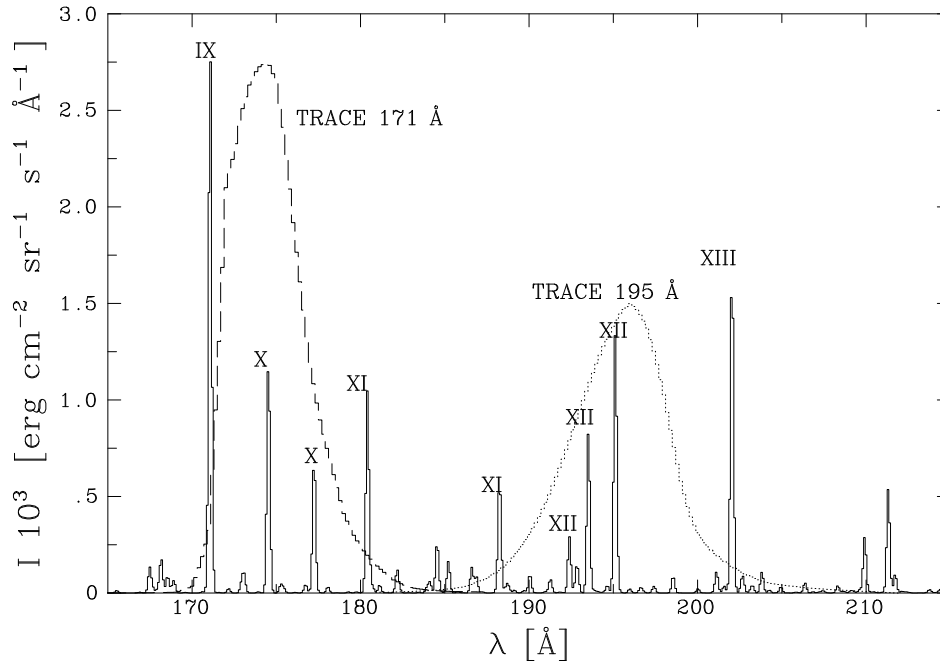


Figure 6. A spectrum derived using a quiet Sun DEM assuming a Maxwellian electron distribution with the strong Fe lines indicated. The weak features at 172 Å and 173 Å originate from O v and O vi. The TRACE 171 Å and 195 Å pass-bands are over-plotted.

Madjarska & Doyle (2002) have already shown that during large bi-directional jets the spectral radiance in chromospheric lines increases by a factor between 1.6 and 2 (using optically thin C I and O I lines). During the present event the radiance increase of the recorded chromospheric lines in terms of line amplitude (assuming as a first approximation that all these lines have the same width) was 2.3 times above the average. Applying this increase to the estimate of the total contribution of the chromospheric lines to Mg x we obtained the registered radiance increase in this line. We conclude that the radiance of the spectral feature at 1249.9 Å is totally due to the blending by the chromospheric lines and therefore Mg x 625 Å has no detectable increase during this very large bi-directional jet.

Fig. 4(d) gives the intensity plot in the TRACE 171 Å window at the SUMER slit position. The integration is done over 2 pixels in the Solar_X dimension and 30 pixels in the Solar_Y dimension, which corresponds to 1'' and 15'', respectively. The strong bi-directional jet is seen in the SUMER spectra that are co-spatial and co-temporal with the TRACE images (as shown in Fig. 1 with the two images showing

this feature marked with an asterisk). Since Mg x is of comparable, although slightly higher formation temperature than Fe ix/x, the bi-directional jet signature in the TRACE 171 Å window is unlikely to be of coronal origin.

4. Non-Maxwellian Electron Distribution

Under ideal thermal equilibrium conditions the electron distribution in a plasma follows a Maxwellian distribution as commonly assumed in the analysis of most solar spectroscopic data. However, non-Maxwellian distributions with an enhanced high-energy tail can occur as a result of high temperature gradients or particle concentration (Owocki & Scudder 1983, Scudder 1992). For example, Maksimovic, Pierrard & Riley (1997) using Ulysses data fitted non-Maxwellian distributions to a series of observed electron velocity distributions.

A convenient parameterization of a non-Maxwellian distribution is the so-called Kappa distribution,

$$f_{\kappa}(E) = \frac{2\sqrt{E}}{\sqrt{\pi}(kT)^{3/2}} A_{\kappa} / \left(1 + \frac{E}{(\kappa - 3/2)kT} \right)^{\kappa+1} \quad (1)$$

where T is the temperature, k the Boltzmann constant and A_{κ} is given in terms of Gamma functions so that

$$A_{\kappa} = \frac{\Gamma(\kappa + 1)}{\Gamma(\kappa - 1/2)(\kappa - 3/2)^{3/2}}. \quad (2)$$

This parameterization represents the Maxwellian distribution at low energy while the parameter κ controls the steepness of the power-law tail, hence, as $\kappa \rightarrow \infty$, the overall distribution becomes Maxwellian.

Dzifčáková (2002a) presented ionization fractions for several Fe ions while Wannawichian, Ruffolo & Kartavyth (2002) give ionization fractions for all ions from C up to Ni. The agreement between the above ionization fraction of Wannawichian, Ruffolo & Kartavyth and those used here is excellent. In Fig. 5 we show the effect of different κ values on the ionization fraction populations of Fe ix and Fe x. It is clear from this figure that for low values of κ , an increasing fraction of Fe ix should occur at non-coronal temperatures.

In Fig. 6 we reproduce the TRACE 171 Å and 195 Å response functions. The above functions range from 170 Å to 210 Å, and contain mostly lines from various Fe ions. For example, the TRACE 171 Å

Table I. Line fluxes for C IV 1548 Å, N V 1238 Å, O VI 1032 Å, Mg X 625 Å, Fe IX 171 Å and Fe X 174 Å for four different bi-directional jets DEM's (see Fig. 7) relative to those derived for the quiet Sun.

DEM	C IV 1548 Å	N V 1238 Å	O VI 1032 Å	Fe IX 171 Å	Fe X 174 Å	Mg X 625 Å
QS	1.00	1.00	1.00	1.00	1.00	1.00
EE1	2.48	4.26	1.26	1.00	1.00	1.00
EE2	5.35	4.70	2.85	1.10	1.00	1.00
EE3	5.51	4.72	3.37	1.20	1.01	1.00
EE4	6.54	4.82	5.07	1.27	1.01	1.00

Table II. Contributions in the TRACE 171 Å pass-band for the different DEM's distribution and departures from a Maxwellian distribution relative to that observed in the quiet Sun for a Maxwellian.

DEM	Maxwellian	Non-Maxwellian			
		$\kappa=10$	$\kappa=5$	$\kappa=3$	$\kappa=2$
QS	1.00	1.00	0.91	0.81	0.80
EE1	1.06	1.00	0.91	0.82	0.80
EE2	1.03	1.03	0.96	0.89	0.86
EE3	1.08	1.08	1.01	0.94	0.91
EE4	1.10	1.10	1.04	0.98	0.95

pass-band is dominated by lines from Fe IX/X while 195 Å is dominated by lines from Fe XII and to a lesser extent Fe XI and Fe XIII as shown by the synthetic spectrum (see Sect. 5 below) produced using the quiet Sun DEM curve of Raymond & Doyle (1981) and the CHIANTI software (Young *et al.* 2003). Dzifčáková (2002b) recently extended the Kappa distribution to the electron excitation rates producing isothermal synthetic spectra for the wavelength range of interest to this study.

5. Synthetic spectra

Before we attempt to calculate model spectra using a non-Maxwellian distribution, we need to check the effect that a DEM distribution suit-

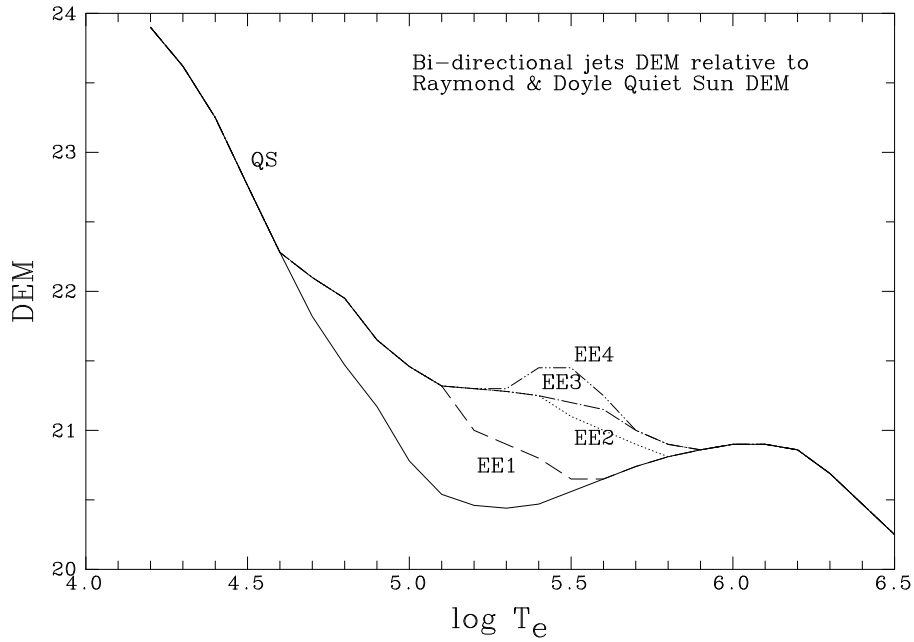


Figure 7. The quiet Sun DEM curve of Raymond & Doyle (1981) plus the four bi-directional jets DEM's used here.

able for a bi-directional jet may have on the TRACE 171 Å and 195 Å pass-bands for a Maxwellian distribution. Based on the observations of Madjarska & Doyle (2002) it is known that the lower chromosphere lines can be enhanced by between 20% and a factor of two during large bi-directional jets while transition lines such as N v 1238 Å are enhanced by factors of 5–6. As shown by Teriaca, Madjarska & Doyle (2002) and confirmed here, coronal lines such as Mg x 625 Å, do not show any evidence of an enhancement during bi-directional jets.

We take as a starting point the DEM curve of Raymond & Doyle (1981) (see Fig. 7), and adjust it at transition region temperatures so as to give the above enhancements factors. In Fig. 7, we show four sample bi-directional jets DEM distributions. Using the CHIANTI database (Young *et al.* 2003), we derive line fluxes for several lines, including C iv 1548 Å, N v 1238 Å, O vi 1032 Å, Mg x 625 Å, Fe ix 171 Å and Fe x 174 Å. (Based on the ionization balance calculations of Mazzotta *et al.* (1998), C iv, N v, O vi, Mg x, Fe ix and Fe x have peak formation temperatures around 100,000 K, 200,000 K, 320,000 K, 1,250,000 K, 800,000 K and 1,000,000 K respectively.) The derived enhancement factors relative to those for the quiet Sun are given in Table I. Here we see that the transition region lines can be enhanced by the required

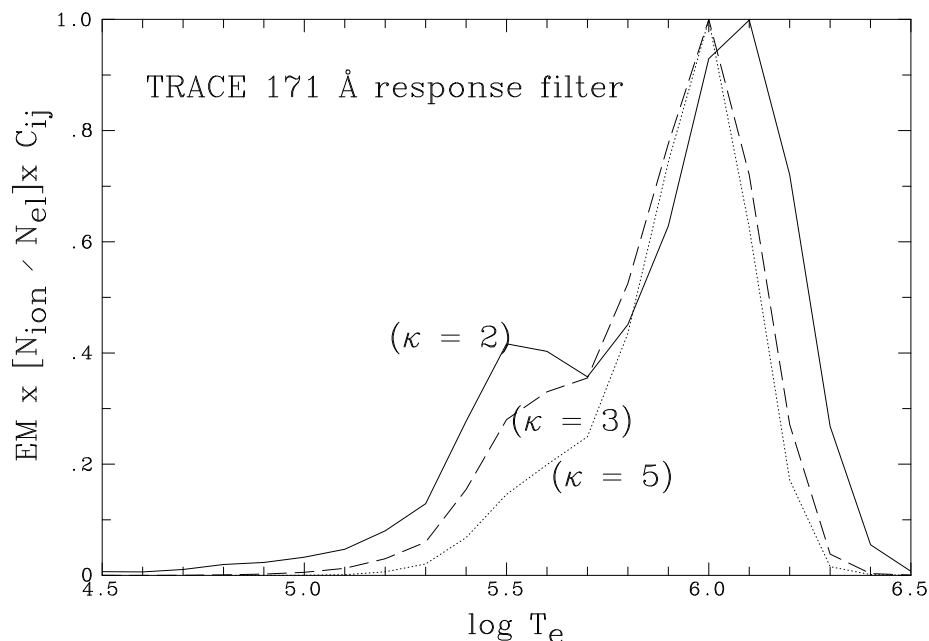


Figure 8. The emissivity response in the TRACE 171 Å pass-band derived by taking the product of the column emission measure times the ionization fraction of Fe IX, Fe X and O VI times the different electron excitation rates for a non-Maxwellian with $\kappa = 2, 3$ & 5, assuming a quiet Sun emission measure and the EE4 emission measure distribution.

factor of 5–6, while Mg X and Fe X are un-affected. The maximum achieved enhancement for Fe IX 171 Å was 1.27 based on the EE4 DEM curve. Within the TRACE 171 Å pass-band, we have a small contribution from O V and O VI lines. Using the quiet Sun DEM curve this amounts to 6% of the strength of the Fe IX 171 Å increasing to 11% using the EE4 DEM distribution.

Using the EE4 DEM curve with a Maxwellian distribution, we obtain only a few percent enhancement in the TRACE 171 Å pass-band (see Table II). Hence, with the ionization balance calculations of Mazzotta *et al.* (1998) and a DEM distribution suitable for bi-directional jets, we can not explain the observed changes in the TRACE 171 Å pass-band as reported in Sect. 3.

Introducing the non-Maxwellian distributions we note (see the first row in Table II) that with the quiet Sun DEM the flux as detected in the TRACE 171 Å pass-band decreases with increasing departure from a Maxwellian. This is because of three factors. First with increasing departure from a Maxwellian the peak in the ionization fraction oc-

curs at lower temperature, secondly with increasing departure from a Maxwellian the electron excitation rate decreases and thus there are fewer excited states and thirdly the emission measure at these lower temperatures is also lower, thus we derive a lower flux. With DEM's more suitable to bi-directional jets, this pattern changes slightly. For example, with the EE3 or EE4 DEM, we see that the flux in the TRACE 171 Å pass-band is approximately a few percent larger than that derived for the quiet Sun model using a κ of 10 or 5, and no increase for smaller κ 's. Adopting a bi-directional jet DEM distribution with a Maxwellian electron distribution gives a small increase in plasma occurring at non-coronal temperatures, however the dominant emission component is still at coronal temperatures. The above would suggest that even with a non-Maxwellian there is little or no change in the flux in the TRACE 171 Å pass-band. This, however, is mis-leading as one must look where the Fe IX lines are formed.

We calculate the emissivity response of the TRACE 171 Å pass-band by calculating synthetic spectra for $\kappa = 2, 3$ & 5, then folding in the TRACE passband to derive the relative contribution of Fe IX, Fe X and O VI using the bi-directional jets DEM distributions. The major effect is that instead of the Fe IX lines being produced at 800,000 to 1,000,000K, it has a significant contribution at lower temperatures.

In the most extreme case ($\kappa = 2$), approximately 12% of the TRACE 171 Å may derive from O V/O VI. With these fractions, the ionization fractions times the column emission measure times the electron excitation rates was derived to give the new TRACE 171 Å pass-band response (see Fig. 8). Thus with a non-Maxwellian electron distribution, a significant fraction of the plasma derives from temperatures around $\approx 300,000$ K.

6. Discussion

As shown in the previous sections, during a bi-directional jet, a fraction of plasma as observed with the TRACE 171 Å pass-band may derive from plasma at transition region temperatures. Since there are between 660 and 3300 bi-directional jets over the surface of the Sun per second, this implies that a significant fraction of plasma may have a non-Maxwellian electron distribution. Doyle & Butler (1985) showed that there was a very close correlation between the rate of flaring activity on a range of late-type stellar objects and the quiescent X-ray emission, and introduced the idea that coronal heating results from flare-like events. Güdel & Benz (1993) extended this to the correlation of radio versus X-ray emission pointing to an intimate connection between the

non-thermal, energetic electrons causing the radio emission and the bulk plasma of the corona responsible for thermal X-rays. The relation was observed over six orders of magnitude. The above interpretation of a large fraction of TRACE 171 Å images sometimes originating from transition region plasma as a result of a non-Maxwellian electron distribution adds further to the connection between non-thermal and thermal processes.

Could this suggest that parts of the corona are heated as a result of a non-Maxwellian distribution in the transition region, with the temperature increase then via a velocity filtration as proposed by Scudder (1992)? It was also suggested that in some instances the excess broadening of transition region lines could be explained by non-Maxwellian distributions as opposed to the commonly accepted view of mass motions. Anderson, Raymond & van Ballegooijen (1996) attempted to test this model by calculating ultra-violet lines intensities for comparison with observational data. They found that the calculated emission measure in the high temperature region (i.e. above 100,000 K) either remained constant or decreased with increasing temperature, being opposite to the observations. However, they also noted that several processes were missing in their calculations.

Recently, several authors (de Pontieu *et al.* 1999, Fletcher & De Pontieu 1999, Martens, Kankelborg & Berger 2000) reported on low-lying (≈ 3000 km) plasma observed in the TRACE 171 Å pass-band. All of these studies assumed the plasma to be coronal. Whether the above non-Maxwellian distributions can explain this low-lying plasma is still an open question but does suggest a possible alternative explanation as to why supposedly coronal material is at such a low altitude. Furthermore, the non-Maxwellian could have implications for the 5 min oscillations seen in TRACE 171 Å images by de Moortel *et al.* (2002). These periods being very similar to those reported by Doyle *et al.* (1998) and Banerjee *et al.* (2001) based on strong transition lines such as O v 629 Å formed around 250,000K. Another possibility are the 3 min sunspots umbral oscillations (Doyle, Dzifčáková & Madjarska 2004) as seen in both TRACE and CDS data. Further work is needed to investigate these aspects.

Acknowledgements

Research at Armagh Observatory is grant-aided by the N. Ireland Dept. of Culture, Arts and Leisure. MM is grateful to PPARC for a postdoctoral fellowship. The SUMER project is financially supported by DLR, CNES, NASA, and PRODEX. This work was supported by PPARC grants PPA/G/S/2002/00020, PPA/V/S/1999/00628 and

PPA/V/S/1999/00668 and by the Programme for Research in Irish Third Level Institutions for Grid-enabled Computational Physics of Natural Phenomena (CosmoGrid). CHIANTI is a collaborative project involving the NRL (USA), RAL (UK), and the Universities of Florence (Italy) and Cambridge (UK).

References

- Anderson, S.W., Raymond, J.C. & van Ballegoijen, A., 1996, *ApJ* 457, 939
 Banerjee, D., O'Shea, E., Doyle, J.G. & Goossens, M., 2001, *A&A* 371, 1137
 Chae, J., Wang, H., Lee, C.Y., Goode, P.R. & Schühle, U., 1998, *ApJ* 497, L109
 Curdt, W., *et al.* 2001, *A&A* 375, 591
 de Moortel, I., Ireland, J., Walsh, R.W. & Hood, A.W., 2002, *Solar Phys.* 209, 61
 Dere K.P., Bartoe J.-D.F., & Brueckner G.E., 1989, *Solar Phys.* 123, 41
 Dere, K.P., 1994, *Adv. Space Res.* 14(4), 13
 de Pontieu, B., Berger, T.E., Schrijver, C.J. & Title, A.M., 1999, *Solar Phys.* 190, 419
 Doyle, J.G. & Butler, C.J., 1985, *Nat* 313, 378
 Doyle, J.G., van den Oord, G.H.J., O'Shea, E. & Banerjee, D., 1998, *Solar Phys.* 181, 51
 Doyle, J.G., Dzifčáková, E. & Madjarska, M.S., 2004, *Solar Phys.* (in press)
 Dzifčáková, E., 2002a, *Solar Phys.* 208, 91
 Dzifčáková, E., 2002b, 'Solar variability: from core to outer frontiers. The 10th European Solar Physics Meeting', ESA SP-506, Vol. 2, p. 597
 Erdélyi, R., De Pontieu, B. & Sarro, L.M., 1999, in *Magnetic Fields and Solar Processes*, Florence, Italy, ESA SP-448, 1345
 Fletcher, L. & de Pontieu, B., 1999, *ApJ* 520, 135
 Güdel, M. & Benz, A.O., 1993, *ApJ* 405, L63
 Innes, D.E., Brekke, P., Germerott, D. & Wilhelm, K., 1997, *Solar Phys.* 175, 341
 Handy, B.N., *et al.* , 1999, *Solar Phys.* 187, 229
 Harrison, R.A., *et al.* 1995, *Sol Phys* 162, 233
 Lemaire, P., *et al.* , 1997, *Solar Phys.* 170, 105
 Madjarska, M.S. & Doyle, J.G., 2002, *A&A* 382, 319
 Maksimovic, M., Pierrard, V. & Riley, P., 1997, *Geo Res Lett* 24, 1151
 Mazzotta, P., Mazzitelli, G., Colafrancesco, S. & Vittorio, N., 1998, *A&A S* 133, 403
 Moses, D. & Cook, J.W., 1994, *Space Sci. Rev.* 70, 81
 Martens, P.C.H., Kankelborg, C.C. & Berger, T.E., 2000, *ApJ* 537, 471
 Owocki, S.P. & Scudder, J.D., 1983, *ApJ* 270, 758
 Pérez, M.E., Doyle, J.G., Erdélyi, R., & Sarro, L.M., 1999, *A&A* 342, 279
 Raymond, J.C. & Doyle, J.G., 1981, *ApJ* 245, 1141
 Ryutova, M.P. & Tarbell, T.D., 2000, *ApJ* 541, L29
 Schrijver, C.J., *et al.* , 1999, *Solar Phys.* 187, 261
 Scudder, J.D., 1992, *ApJ* 398, 319
 Teriaca, L., Madjarska, M.S. & Doyle, J.G., 2002, *A&A* 392, 309
 Wannawichian, S., Ruffolo, D., & Kartavyth, Yu. Yu, 2003, *ApJ S ApJ S* 146, 443
 Winebarger, A.R., Updike, A.C. & Reeves, K.K., 2002, *ApJ* 570, L105
 Wilhelm, K., *et al.* , 1995, *Solar Phys.* 162, 189
 Wilhelm, K., *et al.* , 1997, *Solar Phys.* 170, 75
 Young, P.R., Del Zanna, G., Landi, E., Dere, K.P., Mason, H.E. & Landini, M., 2003, *ApJ S* 144, 135